

## Analysis of an Interface between an Immiscible Polymer Pair by Electron Spectroscopic Imaging

Shin Horiuchi,\*<sup>†</sup> Takeshi Hanada,<sup>†</sup>  
Kiyoshi Yase,<sup>†</sup> and Toshiaki Ougizawa<sup>‡</sup>

National Institute of Materials and Chemical Research,  
1-1 Higashi, Tsukuba, Ibaraki 305-8565, Japan, and  
Department of Organic and Polymeric Materials,  
Tokyo Institute of Technology, Ookayama, Meguro-ku,  
Tokyo 152, Japan

Received July 31, 1998

Revised Manuscript Received December 1, 1998

**Introduction.** Studies on the interfaces between immiscible polymer pairs are quite important with respect to the evaluation of miscibility, adhesion, and bulk properties of polymer blends. Two techniques have been employed to investigate immiscible polymer–polymer interfaces: ellipsometry<sup>1–3</sup> and neutron reflectometry.<sup>4</sup> Both techniques are sensitive to measure the interfacial thickness; however, these cannot provide information on the morphological aspects of the interfacial region.

Energy-filtering transmission electron microscopy (EFTEM) is expected to be one of the most promising techniques for the nanoscale local analysis of materials.<sup>5</sup> EFTEM allows us to analyze elemental compositions by electron energy loss spectroscopy (EELS) and allows us to create elemental distribution images by electron spectroscopic imaging (ESI) with an image processing system, where two-window or three-window methods have been employed to extrapolate the background and to obtain the signals for elemental distributions.<sup>6–8</sup> Some experiments have been carried out in terms of the local analysis around polymer–polymer interfaces using EFTEM. Tremblay et al. introduced an EELS technique to locate an interfacial modifier in a polymer blend.<sup>9</sup> Klotz et al. evaluated the elemental distribution across the interface between a miscible pair of poly(2,6-dimethyl-1,4-phenylene oxide) and polystyrene by the “two-window method” in ESI.<sup>10</sup> In both cases, the signals for the elemental composition across the interfaces were very noisy, resulting in a greater difficulty of the quantitative analysis regarding the interfacial thickness.

We here demonstrate that use of the ESI technique by EFTEM with the aid of the “imaging plate system” (IP) is one of the eligible methods for the investigation of immiscible polymer–polymer interfaces. IP covers a wider dynamic range with better linearity of the signal intensity against the electron dose as compared to conventional photographic films.<sup>11</sup>

The specimen employed in this work is a bilayer specimen of Bisphenol A polycarbonate (PC) and poly(styrene-*co*-acrylonitrile) (SAN). It has been known that PC and SAN are immiscible, but have a favorable interaction.<sup>12</sup> The interfacial thickness between PC and SAN was measured by ellipsometry as functions of temperature and the composition of SAN.<sup>13–15</sup> An

optimum composition of SAN to give maximum interfacial thickness exists in the variation of the interfacial thickness against the acrylonitrile (AN) content in SAN at various temperatures.<sup>16</sup> This suggests that the strong “repulsion effect”<sup>17</sup> between the segments comprising the random copolymer gives rise to the favorable thermodynamic interaction between PC and SAN. In particular, the bilayer specimen of PC and SAN-40, which contains 40 wt % of AN, exhibited extremely thick equilibrium interface at about 40 nm after annealing at 200 °C.<sup>14,15</sup> This evidence encourages us to introduce ESI technique for the identification of such an extremely thick interface.

**Experimental Section. Materials and Specimen Preparation.** PC was supplied by Mitusbishi Gas Chem., of which the  $M_w$  is 37 500 and  $M_w/M_n$  is 1.4. SAN-40 was supplied by Mitsubishi Monsanto, of which the  $M_w$  is 75 800 and  $M_w/M_n$  is 1.9. The bilayer specimen was prepared according to the procedure for ellipsometric analysis.<sup>18</sup> The PC substrate was prepared by melt-pressing between two silicone wafers with a spacer in order to yield an optically flat sheet. Then, the chlorobenzene solution of SAN was coated on a silicone wafer by spin casting, and the SAN film was mounted on the PC substrate by the floating-on-water and pickup method.<sup>1</sup> After drying, the bilayer specimen thus prepared was inserted into a hot chamber kept at 200 °C and was annealed under a nitrogen atmosphere for 30 min. Then it was quenched at ambient temperature and a bilayer specimen consisting of a thin (ca. 300 nm) SAN film and a thick (ca. 0.5 mm) PC substrate with an equilibrium interfacial layer was obtained.

Thin sections from the PC/SAN bilayer specimen were prepared by cutting on a Reichert-Jung Ultracut E microtome with a diamond knife. To ensure that the cutting stroke is perpendicular to the plane of the interface, the optically flat bilayer specimen was clamped with a flat specimen holder, and the holder was set to the specimen arm in order that the arm's stroke should be parallel to the plane of the interface. To avoid the smearing the interface structure, the cutting stroke goes along the interface. The speed and the thickness for the cut were set to 1 mm/s and to 50 nm, respectively, and gray-colored specimens were collected on a 600 meshes copper grid.

**Energy-Filtering Transmission Electron Microscopy (EFTEM) and Image Processing.** A Carl Zeiss EM902 equipped with a Casting-Henry filter lens was operated at 80 kV. To avoid irradiation damage and heating of the specimens by the incident electron beam, observation was carried out cryogenically at 100 K. Electron spectroscopic images (ES images) were observed with an energy width of 20 eV, and the magnification was set at 50 000. ES images at selective energy loss levels were exposed on IPs at an acquisition time from 1 to 2 s. Electron energy loss spectra (EEL spectra) in selective energy loss levels were also recorded on IPs. The area in a specimen was selected by the selection aperture locating just above the filter. A spectrum with the energy width of about 120 eV can be captured on a single IP. The reading out of exposed IPs was carried out by a FDL5000 imaging plate system (Fuji Photo Film), where the reading pixel size is 25 × 25 μm and the signal intensity is digitized into 14 bits gray levels.

\* To whom correspondence should be addressed. Telephone: 81-298-54-6321. Fax: 81-298-54-6232. E-mail: shoriuchi@nimc.go.jp.

<sup>†</sup> National Institute of Materials and Chemical Research.

<sup>‡</sup> Tokyo Institute of Technology.

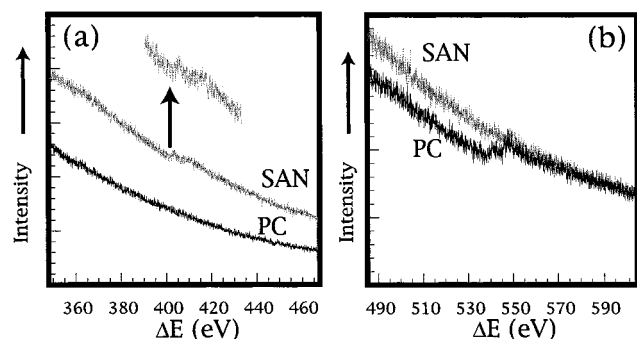


**Figure 1.** EEL spectra taken from the PC substrate and from the SAN-40 layer. Part a shows the nitrogen core loss peak from the SAN-40 layer, and part b shows the oxygen core loss peak from the PC substrate.

Image processing was carried out by use of L-Process, Image Gauge (Fuji Photo Film), and Adobe Photoshop 4.0.

**Results and Discussion.** EEL-spectra were taken from the both layers in the specimen in various energy loss levels. First, the low loss region including the zero loss and plasmon loss peaks were taken, and the homogeneity in terms of the specimen thickness was evaluated. The ratio of the integration of the zero loss to the plasmon loss peaks corresponded to the relative local thickness.<sup>19</sup> Through this evaluation, no appreciable difference in thickness across the interface was qualitatively shown.

In Figure 1, the EEL spectra recorded from the PC and the SAN-40 areas with the diameter of about 100 nm are given. Figure 1a shows the spectra in the energy loss region between 340 and 460 eV, where one can detect the nitrogen K-edge at 400 eV in the spectrum taken from the SAN layer. On the other hand, the spectrum taken from the PC substrate exhibited the oxygen K-edge at around 535 eV as shown in Figure 1b. The detectable core loss peaks are quite weak and noisy, which is particular in the nitrogen core loss peak. Therefore, this implies the difficulty of the quantitative analysis of the interfacial region by EELS.

Thus, we employed the ESI mode in EFTEM, and carbon, nitrogen and oxygen elemental distribution images of the PC/SAN-40 bilayer specimen were created according to the "three-window method".<sup>20</sup> In this method, the background intensity in a EEL spectrum,  $S(E)$ , is assumed to have an inverse power-law dependence on energy loss,  $E$ , as follows:

$$S(E) = AE^{-r} \quad (1)$$

where the constant factors  $A$  and  $r$  are calculated pixel by pixel from the signals at two energy windows below the core loss edge. Then the background is extrapolated

to the edge, and an elemental distribution image can be obtained by the subtraction of the background image from the core loss image.<sup>21</sup>

For the imaging of the carbon distribution, two ES images formed by electrons with an energy loss of  $250 \pm 10$  and  $270 \pm 10$  eV are used to create the background image, and then, the background image is subtracted from the carbon core loss image formed by electrons with an energy loss of  $295 \pm 10$  eV. The nitrogen and the oxygen distribution images are obtained by the same procedure: for the nitrogen distribution image, three energy windows at  $360 \pm 10$ ,  $385 \pm 10$ , and  $410 \pm 10$  eV are selected; for the oxygen distribution image,  $490 \pm 10$ ,  $515 \pm 10$ , and  $545 \pm 10$  eV are selected. Figure 2 shows the three elemental distribution images thus created from the same position of the specimen. The carbon distribution image exhibits no remarkable contrast between the PC and the SAN-40 sides due to the comparable carbon concentrations in the two polymers. However, the SAN-40 layer is slightly brighter than the PC substrate, which correctly reflects the difference in the carbon concentration between the two polymers. The nitrogen distribution image exhibits the SAN-40 layer as a brighter area, and the oxygen distribution image exhibits the PC substrate as a brighter area. In the nitrogen distribution image, all pixels in the PC substrate should be zero in gray level in principle, however, some pixels remain bright. The same tendency is shown in the oxygen distribution image. The weak core loss peaks and the high background intensity in the EEL spectra as shown in Figure 1 may cause such an inaccuracy in the process of the "three-window method".

From the elemental distribution images shown in Figure 2, the gray value profiles along a line perpendicular to the interface are evaluated, which are equivalent to the concentration of the respective elements across the interface. Figure 3 shows the gray value profiles along the lanes indicated in Figure 2. The width of the lanes is 50 nm, which is corresponded to 100 pixels in a IP. Thus, the gray-level profiles obtained from the lanes are corresponded to the average of the 100 traces along the line perpendicular to the interface in the lanes. The profiles shown in Figure 3a includes the PC substrate, the SAN-40 thin layer and the blank region. Although the profiles are noisy, they show the steep gradients at the interface. Nitrogen and oxygen should be coexist in the interfacial region; hence, the interfacial region is defined as indicated in Figure 3b, where the intensity profiles of Figure 3a are magnified, focusing on the interfacial region, and then, the interfacial thickness is estimated at about 40 nm. This value is close to the one measured by ellipsometry.<sup>14,15</sup>

The spectra shown in Figure 1 suggest the limitation of EELS for the local analysis of the interface because even the spectra taken from the large area (ca. 100 nm

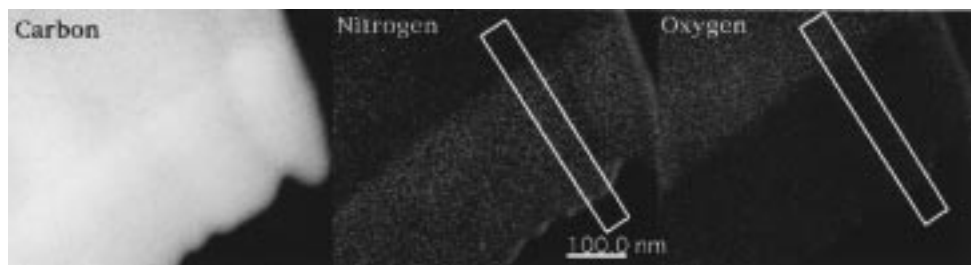


**Figure 2.** Carbon, nitrogen and oxygen distribution images of a PC/SAN-40 bilayer specimen created by the "three-window method".



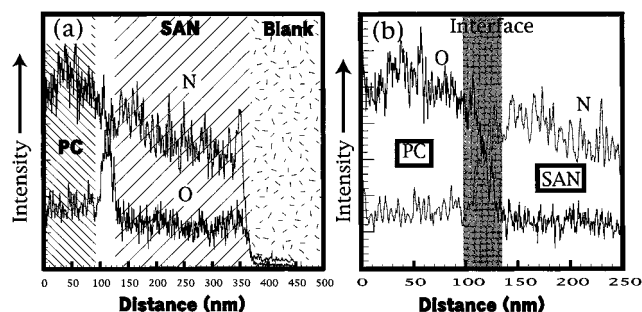


**Figure 3.** (a) Intensity profiles along the line perpendicular to the PC/SAN-40 interface obtained from the nitrogen and the oxygen distribution images. The area for the profiles are indicated in Figure 2 as lanes with the width of 50 nm. (b) Magnified view of part a, focusing on the interfacial region.

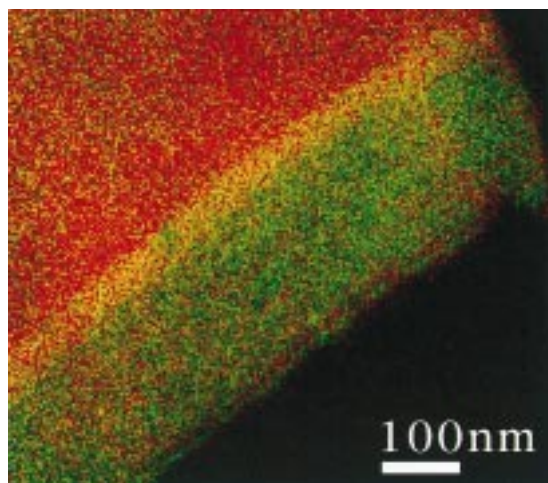


**Figure 4.** A RGB composite of the nitrogen and the oxygen distribution images: red, nitrogen (PC substrate); green, oxygen (SAN-40 layer); yellow, interfacial layer.

in diameter) are quite noisy. On the other hand, the ESI technique enables us to perform local analysis of the interfacial region. The profiles from wider lane across the interface give smooth profiles and clearly show the interfacial thickness, while narrower lanes give noisier profiles and make it difficult to detect the interfacial area. This indicates that the resolution of this method for our specimen is around 50 nm. However, by overlapping the nitrogen and the oxygen distribution images at the same positions in the specimen, the cross sectional view of the interfacial layer can be imaged, and we can see the thickness and the geometry of the interfacial layer simultaneously in an image.

First, nitrogen and oxygen distribution images which are expressed by 14 bits gray level colors are translated to the color images composed of three planes of pixels where each pixel has red, green and blue intensities, each coded on 8 bits (RGB mode). Then, those images are decomposed into the primary RGB color components. Afterward, one color plane is extracted in each images with distinct colors, and the two extracted images are composed again, precisely overlapped at the same positions of the specimen. Thus, the interfacial region can be visualized as the yellowish area due to the composition of green and red pixels in the two images

as shown in Figure 4. This reveals that the interfacial layer is relatively flat and parallel and is about 40 nm in thickness.

The interfacial thickness estimated at about 40 nm is much larger than theoretically predictable values and the coil size of the component polymers. But such extremely thick interfaces have been also attained in a poly(methyl methacrylate) (PMMA)/SAN immiscible system<sup>3</sup> and a polyamide/poly(styrene-*co*-maleic anhydride) reactive system by ellipsometric analysis.<sup>22</sup> The results obtained by the ESI technique here support the credibility of the ellipsometric measurements. In future, we will apply the ESI technique to the investigation of interfaces in blend materials. For ellipsometry and neutron reflectometry a specimen should be served as a bilayer specimen, where a interface is set up between two polymer layers. On the other hand, ESI would make it possible to compare the results obtained from a bilayer specimen with those obtained from a bulk blend specimen.

## References and Notes

- (1) Yukioka, S.; Inoue, T. *Polym. Commun.* **1991**, *32*, 17.
- (2) Higashida, N.; Kressler, J.; Yukioka, S.; Inoue, T. *Macromolecules* **1992**, *25*, 5259.
- (3) Yukioka, S.; Inoue, T. *Polymer* **1993**, *34*, 1256.
- (4) Fernandez, M. L.; Higgins, J. S.; Penfold, J.; Ward, R. C.; Shackleton, C.; Walsh, D. J. *Polymer* **1988**, *29*, 1923.
- (5) Brown, L. M. *Nature* **1993**, *366*, 721.
- (6) Kunz, M.; Moller, M.; Heinrich, U. R.; Cantow, H. J. *Makromol. Chem., Macromol. Symp.* **1989**, *23*, 57.
- (7) Cantow, H. J.; Kunz, M.; Klotz, S.; Moller, M. *Makromol. Chem., Macromol. Symp.* **1989**, *26*, 191.
- (8) Horiuchi, S.; Yase, K.; Kitano, T.; Higashida, N.; Ougizawa, T. *Polym. J.* **1997**, *29*, 380.
- (9) Tremblay, A.; Tremblay, S.; Favis, B. D.; Selmani, A.; L'Esperance, G. *Macromolecules* **1995**, *28*, 4771.
- (10) Klotz, S.; Seggern, J.; Kunz, M.; Cantow, H. J. *Polym. Commun.* **1990**, *31*, 332.
- (11) Mori, N.; Oikawa, T.; Harada, Y.; Miyahara, J. *J. Electron Microsc.* **1990**, *39*, 433.
- (12) Callaghan, T. A.; Takakura, K. Paul, D. R.; Padwa, A. R. *Polymer* **1993**, *34*, 3796.
- (13) Funaki, S.; Higashida, N.; Inoue, T. *Polym. Prepr., Jpn.* **1994**, *43*, 2922.
- (14) Li, H.; Fujitsuka, R.; Yang, Y.; Ougizawa, T.; Inoue, T. *Prepr. 6th SPSJ Intern. Polym. Conf.* **1997**, 48.
- (15) Li, H.; Yang, Y.; Fujitsuka, R.; Ougizawa, T.; Inoue, T. *Polymer*, in press.
- (16) The dependence of the interfacial thickness on the AN content of SAN was measured at various temperatures from 180 to 215 °C. A maximum thickness was attained at around 25 wt % of SAN at 180 °C and was attained at 40 wt % at 200 °C.
- (17) Suess, M.; Kressler, J.; Kammer, H. W. *Polymer* **1987**, *28*, 957.
- (18) Yukioka, S.; Nagato, K.; Inoue, T. *Polymer* **1992**, *33*, 1171.
- (19) Egerton, R. F.; Leapman, R. D. *Energy-Filtering Transmission Electron Microscopy*; Reimer, L., Ed.; Springer Verlag: Berlin, Heidelberg, Germany, 1995; p 285.
- (20) Reimer, L. *Energy-Filtering Transmission Electron Microscopy*; Reimer, L., Ed.; Springer Verlag: Berlin, Heidelberg, Germany, 1995; p 384.
- (21) To simplify the intra-images calculation, the signal intensities recorded on IPs are translated to logarithmic values, and the double logarithmic form of the eq 1,  $\log S(E) = \log A - r \log E$ , was applied for the creation of the background image.
- (22) Yukioka, S.; Inoue, T. *Polymer* **1994**, *35*, 1182.

MA981200M